Supporting Information (SI)

π-conjugated organic molecule modified strategy to achieve high-performance metal nitrate birefringent crystal

Yi-Lei Lv, Liang Ma, Guo-Ren Zhu, Bing-Wei Miao, Wenlong Liu, Sheng-Ping Guo* and Ru-Ling Tang*

†School of Chemistry and Chemical Engineering, Yangzhou University, Yangzhou, Jiangsu 225002, P. R. China

Corresponding author: rltang@yzu.edu.cn, spguo@yzu.edu.cn

Supporting Information Index

Tables and Figures

Table S1. Crystal data and structure refinement parameters for $Hg_3O_2(NO_3)_2 \cdot H_2O$ and $(CH_5N_3S)_2Hg(NO_3)_2$.

Empirical formula	**$Hg_3O_2(NO_3)_2 \cdot H_2O$**	**$(CH_5N_3S)_2Hg(NO_3)_2$**
Formula weight	775.81	506.89
Temperature/K	296	296
Crystal system	triclinic	monoclinic
Space group	$P\bar{1}$	$C2/c$
a/Å	6.9108(3)	11.6751(7)
b/Å	6.9443(3)	13.5050(8)
c/Å	10.1264(5)	20.7268(12)
α(°)	99.946(2)	90
β(°)	97.884(2)	100.495(2)
γ(°)	119.581(2)	90
Volume/Å^3	402.00(3)	1226.37(10)
Z	2	4
ρcalc g/cm^3	6.049	2.745
μ/mm^{-1}	57.181	12.931
F(000)	656.0	952.0
Radiation	MoKα (λ = 0.71073)	MoKα (λ = 0.71073)
2Θ range for data collection/°	6.049 to 50.052	5.762 to 54.978
Index ranges	-8 ≤ h ≤ 8,-8 ≤ k ≤ 8,-12 ≤ l ≤ 12	-14 ≤ h ≤ 11, -9 ≤ k ≤ 9, -18 ≤ l ≤ 18
Reflections collected	656.0	6132
Independent reflections	1424 [R_{int} = 0.0429, R_{sigma} = 0.0328]	1402 [R_{int} = 0.0363, R_{sigma} = 0.0362]
Data/restraints/parameters	1424/6/131	1402/0/88
Goodness-of-fit on F^2	1.066	1.019
Final R indexes [I ≥ 2σ (I)] [a,b]	R_1=0.0181, WR_2=0.0416	R_1=0.0229, WR_2=0.0325
Final R indexes [all data][a,b]	R_1=0.0203, WR_2=0.0423	R_1=0.0361, WR_2=0.0348

[a]$R_1 = \sum||F_o| - |F_c||/\sum|F_o|$ and [b]$wR_2 = [w (F_o^2 - F_c^2)^2/wF_o^4]^{1/2}$ for $F_o^2 > 2\sigma (F_o^2)$

Table S2. Important bond lengths (Å) and bond angles (°) for $Hg_3O_2(NO_3)_2·H_2O$ and $(CH_5N_3S)_2Hg(NO_3)_2$.

Bond Length(Å)		**$Hg_3O_2(NO_3)_2·H_2O$**	
Hg(1)—O(1)[2]	2.070(5)	Hg(2)[1]—O(2)	2.081(4)
Hg(1)—O(2)	2.072(5)	N(1)—O(3)	1.269(7)
Hg(2)—O(1)	2.065(4)	N(1)—O(4)	1.254(7)
Hg(2)—O(2)[4]	2.081(4)	N(1)—O(5)	1.216(7)
Hg(3)—O(1)	2.058(4)	N(2)—O(7)	1.243(8)
Hg(3)—O(2)	2.057(5)	N(2)—O(8)	1.241(8)
Hg(1)[3]—O(1)	2.070(5)	N(2)—O(9)	1.210(9)
Bond Angles (deg)		**$Hg_3O_2(NO_3)_2·H_2O$**	
O(1)[2]—Hg(1)—O(2)	175.00(18)	O(5)—N(1)—O(4)	121.1(6)
O(1)—Hg(2)—O(2)[3]	171.87(18)	O(8)—N(2)—O(7)	119.5(7)
O(2)—Hg(3)—O(1)	177.83(18)	O(9)—N(2)—O(7)	120.6(7)
O(4)—N(1)—O(3)	118.5(6)	O(8)—N(2)—O(8)	119.9(7)
O(5)—N(1)—O(3)	120.3(6)		

Symmetry transformations used to generate equivalent atoms:[1]1+X,+Y,+Z; [2]1+X,1+Y,+Z; [3]-1+X,+Y,+Z; [4]-1+X,-1+Y,+Z

Bond Length(Å)		**$(CH_5N_3S)_2Hg(NO_3)_2$**	
Hg(1)—S(1)[1]	2.3686(8)	O(1)—N(1)	1.250(4)
Hg(1)—S(1)	2.3686(8)	O(2)—N(1)	1.242(3)
Hg(1)—N(2)[1]	2.496(3)	N(1)—O(3)	1.214(3)
Hg(1)—N(2)	2.496(3)	N(3)—C(1)	1.322(4)
S(1)—C(1)	1.719(3)	N(4)—C(1)	1.315(4)
Bond Angles (deg)		**$(CH_5N_3S)_2Hg(NO_3)_2$**	
S(1)[1]—Hg(1)—S(1)	157.01(5)	O(3)—N(1)—O(1)	119.5(3)
S(1)[1]—Hg(1)—N(2)	114.03(7)	O(3)—N(1)—O(2)	120.4(3)
S(1)—Hg(1)—N(2)[1]	114.03(7)	N(3)—N(2)—Hg(1)	108.30(18)
S(1)[1]—Hg(1)—N(2)[1]	79.23(7)	C(1)—N(3)—N(2)	123.4(3)
S(1)—Hg(1)—N(2)	79.23(6)	N(3)—C(1)—S(1)	125.5(2)
N(2)[1]—Hg(1)—N(2)	112.88(12)	N(4)—C(1)—S(1)	116.7(2)

C(1)—S(1)—Hg(1)	101.64(11)	N(4)—C(1)—N(3)	117.8(3)
O(2)—N(1)—O(1)	120.1(3)		

Symmetry transformations used to generate equivalent atoms:[1]1-*x*,+*y*,3/2-*z*

Table S3. Fractional atomic coordinates (× 10^4) and equivalent isotropic displacement parameters (Å^2 × 10^3) for $Hg_3O_2(NO_3)_2 \cdot H_2O$. Ueq is defined as 1/3 of the trace of the orthogonalized Uij tensor.

atom	Wyckoff site	*x*	*y*	*z*	U_{eq}[a]/Å^2
Hg(1)	2*i*	9062.9(4)	10032.2(4)	2042.7(3)	12.66(10)
Hg(2)	2*i*	-915.8(4)	5071.7(4)	2103.8(3)	14.94(11)

Hg(3)	2*i*	4054.4(4)	4996.3(4)	1917.4(3)	15.62(11)
O(1)	2*i*	988(7)	3589(8)	2473(5)	17.0(11)
O(2)	2*i*	7185(8)	6459(8)	1440(5)	16.7(11)
O(3)	2*i*	2358(9)	10434(8)	757(5)	21.8(11)
O(4)	2*i*	2328(9)	7292(8)	740(5)	24.8(12)
N(1)	2*i*	3434(10)	9451(10)	1040(6)	12.7(12)
O(5)	2*i*	5495(8)	10589(9)	1578(5)	25.2(12)
O(6)	2*i*	6624(13)	4448(13)	3972(7)	45.4(17)
O(7)	2*i*	12223(10)	9601(11)	3605(6)	38.3(15)
N(2)	2*i*	12436(11)	9852(11)	4872(6)	23.8(16)
O(8)	2*i*	14216(12)	11522(12)	5705(7)	53.8(19)
O(9)	2*i*	10942(14)	8462(14)	5297(8)	73(2)

Table S4. Fractional atomic coordinates (× 10^4) and equivalent isotropic displacement parameters (Å^2 × 10^3) for $(CH_5N_3S)_2Hg(NO_3)_2$. Ueq is defined as 1/3 of the trace of the orthogonalized Uij tensor.

atom	Wyckoff site	*x*	*y*	*z*	U_{eq}[a]/Å^2
Hg(1)	4*e*	5000	2829.1(3)	7500	35.87(10)
S(1)	8*f*	5523.8(8)	2214.3(12)	6012.5(6)	34.0(2)
O(1)	8*f*	2739(2)	640(3)	6898.4(18)	47.7(7)
O(2)	8*f*	3310(2)	-1026(3)	5853.6(17)	47.0(7)
N(1)	8*f*	3237(2)	-723(4)	6690(2)	31.6(7)
N(2)	8*f*	3482(2)	4627(3)	6435.7(18)	33.1(7)
N(3)	8*f*	3502(2)	4142(3)	5494.5(17)	31.0(7)
N(4)	8*f*	4272(3)	2791(3)	4343.7(19)	38.9(7)
O(3)	8*f*	3642(3)	-1747(4)	7309.9(19)	66.8(9)
C(1)	8*f*	4335(3)	3121(4)	5249(2)	25.5(7)

Table S5. The reported metal nitrate birefringent crystals. ("Si" means the file is in the Supporting Information)

Compounds	**Space group**	**Birefringence**	**Ref.**
$Sc(IO_3)_2(NO_3)$	*R*32	Exp.0.348@546nm	Si1
$Hg_3(TeO_3)(Te_3O_7)(NO_3)_2$	*Pnma*	Exp.0.295@546nm	41
$K(H_3C_3N_3O_3)(NO_3)$	$P2_1/c$	Cal.0.253@546.1nm	Si2
$Pb_2(NO_3)_2(H_2O)F_2$	*Amm*2	Cal.0.230@1064nm	Si3
$Hg_3O_2(NO_3)F$	*Pbca*	Cal.0.230@1064nm	40c
$Rb(H_3C_3N_3O_3)(NO_3)$	$P2_1/c$	Cal.0.224@546.1nm	Si2
$Gu_2Bi(NO_3)_3Cl_2$	$P2_1/c$	Exp.0.186@546nm	Si4
$Pb_2(BO_3)(NO_3)$	$P6_3mc$	Cal.0.174@1064nm	18
$Hg_{16}(NO_3)_6O_{12}F_2(H_2O)$	*Ibca*	Exp.0.17@546nm	40d
$(NH_4)_3SbF_4(NO_3)_2$	*Pnma*	Cal.0.164@546nm	19
$Gu_3Bi_2NO_3Cl_8$	$P\bar{1}$	Exp.0.162@546nm	Si4
$Cs_2Pb(NO_3)_2Br_2$	$I4_1/amd$	Exp.0.147@546nm	20
$La(OH)_2NO_3$	$P2_1$	Exp.0.146@589.6nm	Si5
$CsHgNO_3Cl_2$	$P6_3/mmc$	Exp.0.145@ 546nm	40b
$Na_3Rb_6(CO_3)_3(NO_3)_2Cl\cdot(H_2O)_6$	$P6_3/mcm$	Exp. 0.14@546nm	Si8
$Y(OH)_2NO_3$	$P2_1$	Exp.0.133@589.6nm	Si5
$Bi_3TeO_6OH(NO_3)_2$	$P2_1$	Cal.0.115@1064nm	21
$Gd(OH)_2NO_3$	$P2_1$	Exp.0.112@589.6nm	Si5
$K_2Hg(NO_3)_4$	$I\bar{4}2m$	Exp.0.107@546nm	Si7
$Rb_2Hg(NO_3)_4$	$I\bar{4}2m$	Exp.0.092@546nm	Si7
$(NH_4)_3SbF_3(NO_3)_3$	$P2_1$	Cal.0.098@546nm	19
$Ba_2NO_3(OH)_3$	$P\bar{6}2m$	Cal.0.082@532nm	Si8
$(C_8H_6BrN_2O)NO_3$	*Cc*	Cal.0.08@550nm	Si9
$Sr(NO_3)(NH_2SO_3)\cdot H_2O$	$Pca2_1$	Cal.0.0665@532nm	Si10
$Rb_2SbF_3(NO_3)_2$	$P2_1$	Cal.0.06@1064 nm	Si11
$PbCdF(SeO_3)(NO_3)$	$Pca2_1$	Cal.0.055@1064nm	Si12
$RbSnF_2NO_3$	*C*2/*m*	Cal.0.05@1064nm	Si11

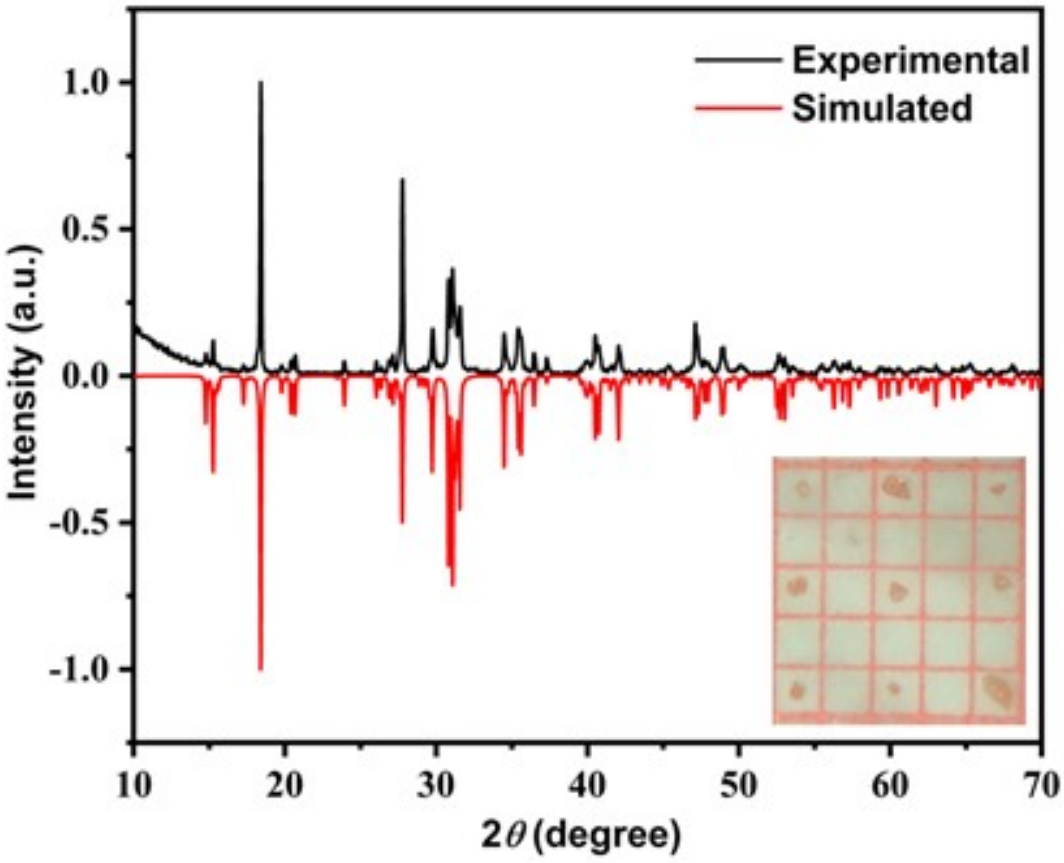

Figure S1. Experimental and simulated powder XRD patterns of $Hg_3O_2(NO_3)_2 \cdot H_2O$ (1 grid = 1 mm).

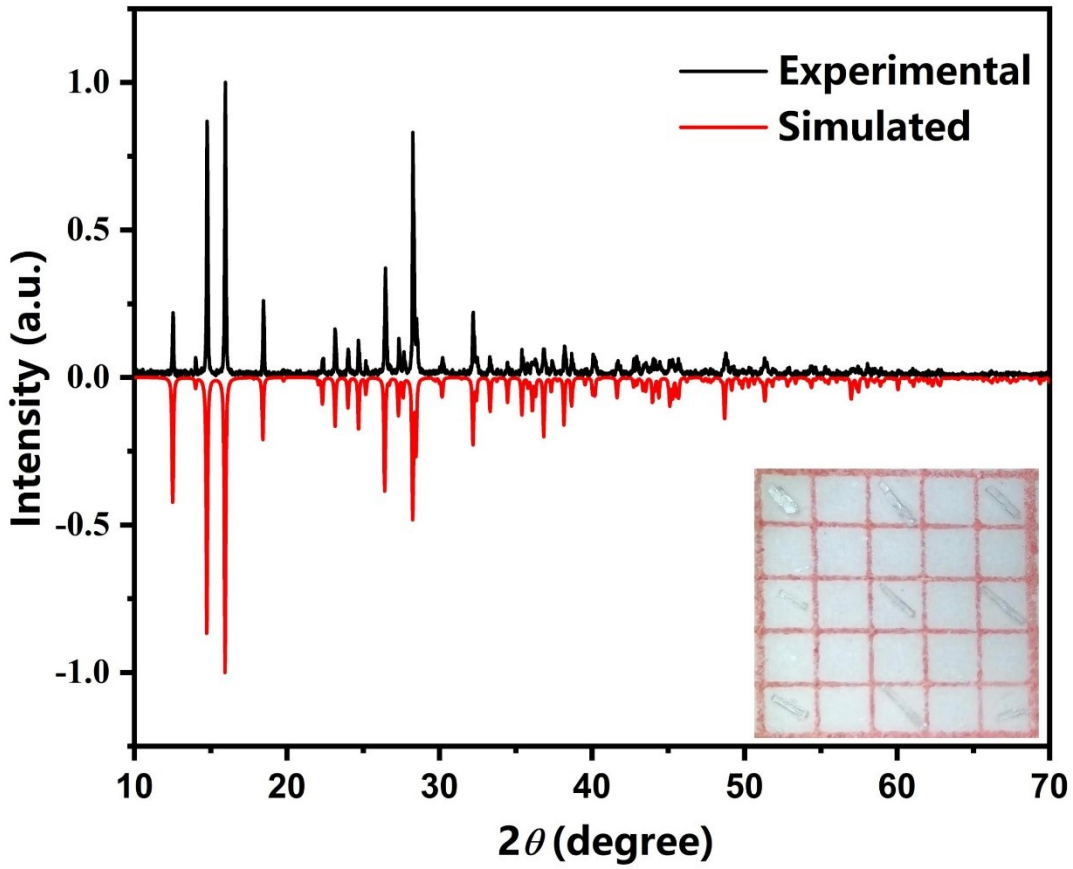

Figure S2. Experimental and simulated powder XRD patterns of $(CH_5N_3S)_2Hg(NO_3)_2$ (1 grid = 1 mm).

(a)

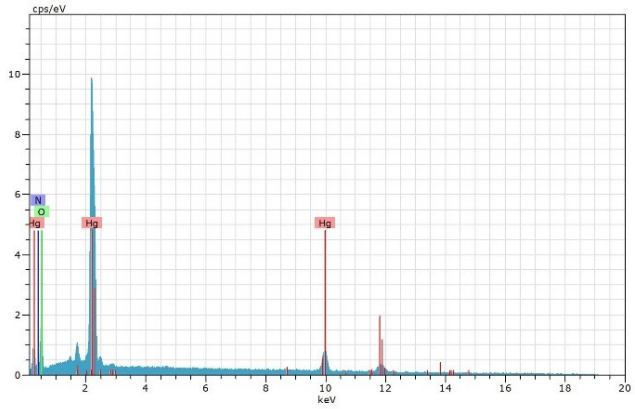

The molar ratio of Hg : O : N from the EDS results.

Compound		Molar ratio
1	Hg : O : N	21.83 : 63.91 : 14.27 = 3.06 : 8.96 : 2
2	Hg : O : N	21.56 : 64.26 : 14.18 = 3.04 : 9.06 : 2
3	Hg : O : N	21.56 : 64.17 : 14.28 = 3.02 : 8.99 : 2

(b)

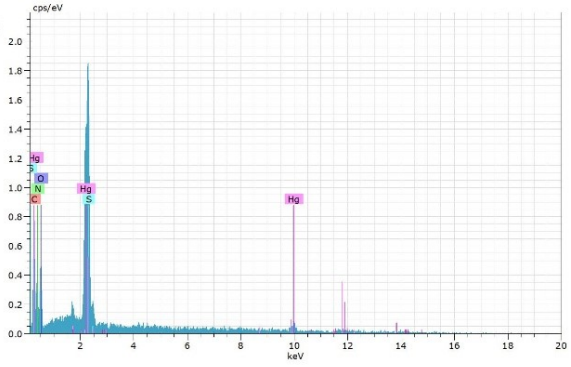

The molar ratio of Hg : O : N : S : C from the EDS results.

Compound		Molar ratio
1	Hg : O : N : S : C	5.26 : 31.57 : 42.1 : 10.53 : 10.54=1 : 6 : 8 : 2 : 2
2	Hg : O : N : S : C	5.26 : 32.09 : 41.82 : 10.52 : 10.31=1 : 6.1 : 7.95 : 2 : 1.96
3	Hg : O : N : S : C	5.3 : 32.06 : 42.93 : 10.34 : 9.37=1 : 6.05 : 8.1 : 1.95 : 1.8

Figure S3. EDS image and data for $Hg_3O_2(NO_3)_2 \cdot H_2O$ (a) and $(CH_5N_3S)_2Hg(NO_3)_2$ (b).

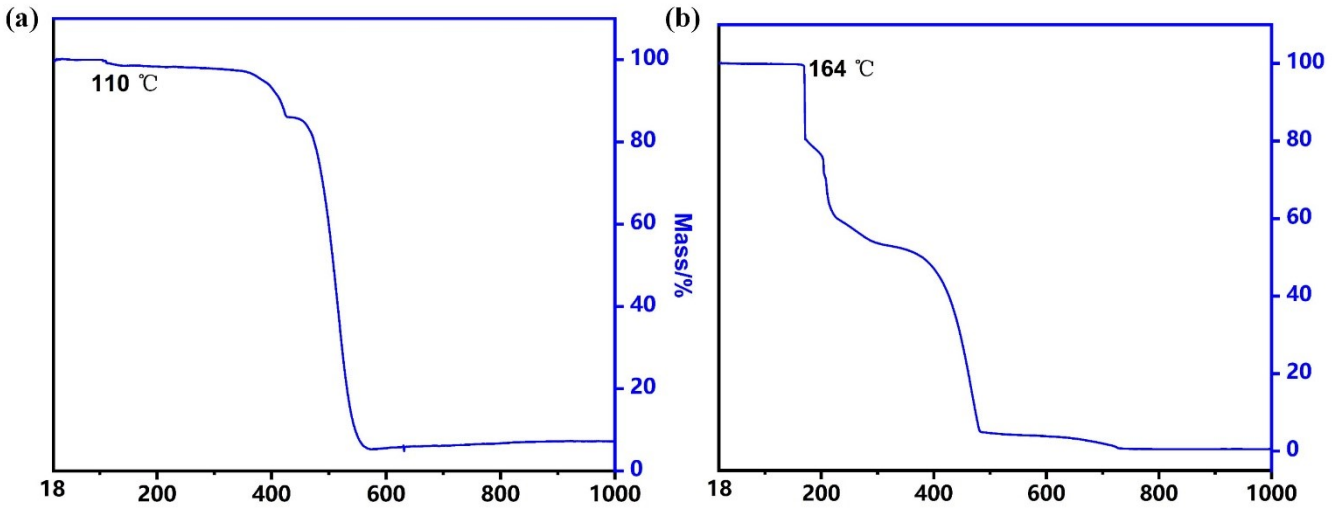

Figure S4. TG curves of $Hg_3O_2(NO_3)_2 \cdot H_2O$ (a) and $(CH_5N_3S)_2Hg(NO_3)_2$ (b).

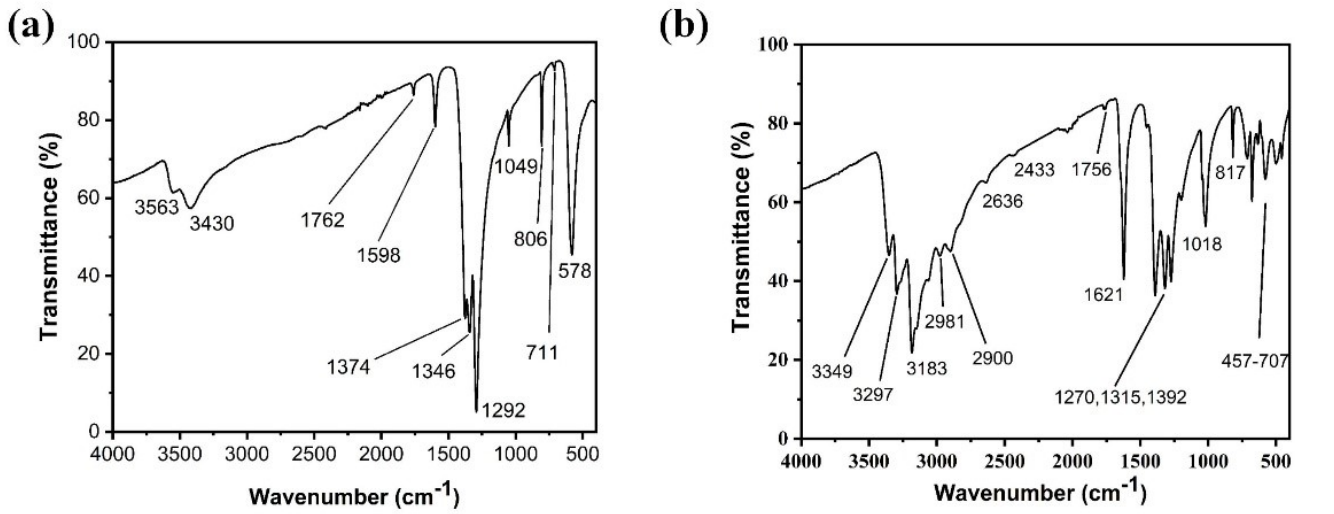

Assignment (cm^{-1})	$Hg_3O_2(NO_3)_2 \cdot H_2O$
V(O-H)	3563, 3430, 1762, 1598
V(N-O)	1374, 1346, 1292, 1049, 806
V(Hg-O)	711, 578

Assignment (cm^{-1})	$(CH_5N_3S)_2Hg(NO_3)_2$
V(N-H)	3349-2900, 1018
V(C-N)	2636, 2433
V(N-C-N)	1756, 1621
V(C=S)	1398, 817
V(N-O)	1392, 1315, 1270
V(S-Hg-S) and *V*(Hg-N)	707-457

Figure S5. IR spectrum and the peaks' assignment for $Hg_3O_2(NO_3)_2 \cdot H_2O$ (a) and $(CH_5N_3S)_2Hg(NO_3)_2$ (b).

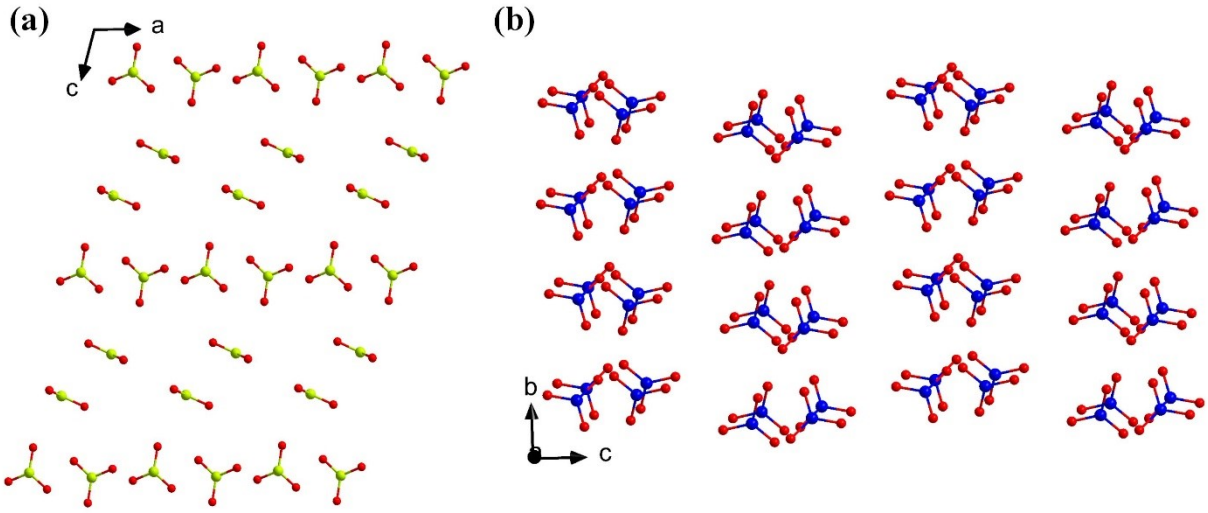

Figure S6. The arrangement of NO_3^- for $Hg_3O_2(NO_3)_2 \cdot H_2O$ (a) and $(CH_5N_3S)_2Hg(NO_3)_2$ (b).

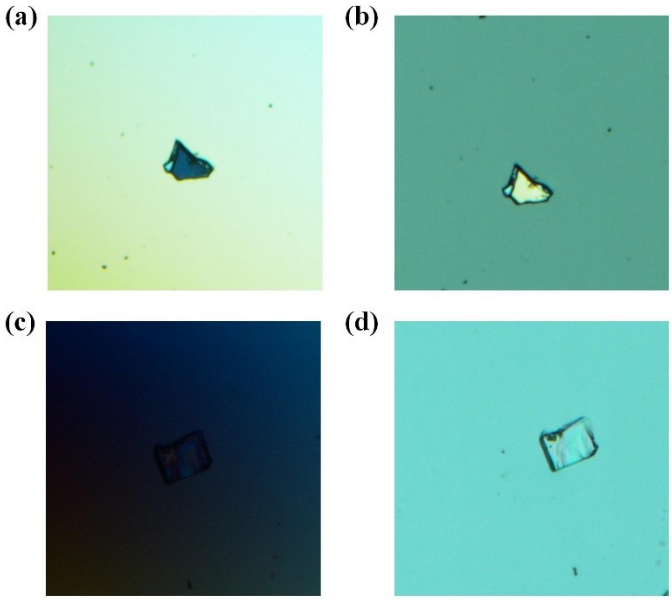

Figure S7. (a) Original single crystal polarized optical microscope image and (b) A single crystal corresponding to complete extinction for $Hg_3O_2(NO_3)_2 \cdot H_2O$; (c) Original single crystal polarized optical microscope image and (d) A single crystal corresponding to complete extinction for $(CH_5N_3S)_2Hg(NO_3)_2$.

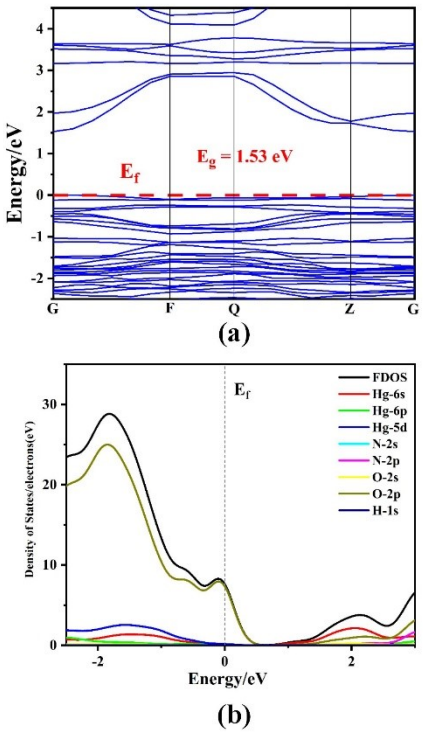

Figure S8. (a) Calculated band gap and (b) Density of states (DOS) for $Hg_3O_2(NO_3)_2 \cdot H_2O$.

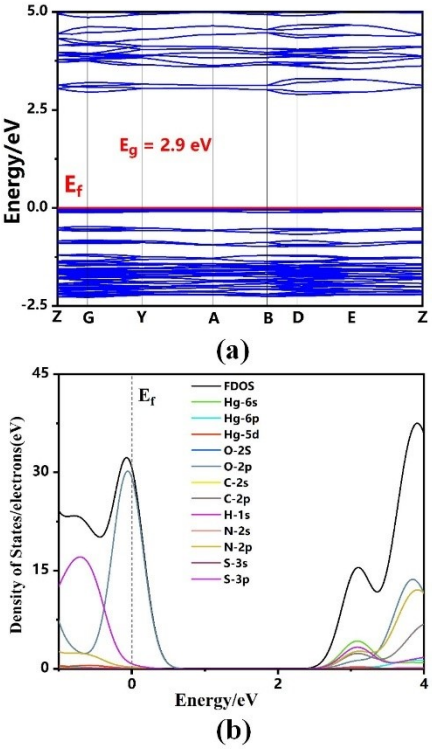

Figure S9. (a) Calculated band gap and (b) Density of states (DOS) for $(CH_5N_3S)_2Hg(NO_3)_2$.

References:

1. C. Wu, X. X. Jiang, Z. J. Wang, L. Lin, Z. S. Lin, Z. P. Huang, X. F. Long, M. G. Humphrey, C. Zhang, Giant Optical Anisotropy in the UV-Transparent 2D Nonlinear OpticalMaterial $Sc(IO_3)_2(NO_3)$, *Angew. Chem. Int. Ed.,* 2021, **60**, 3464–3468.
2. X. Hao, M. Luo, C. S. Lin, G. Peng, T. Yan, D. H. Lin, L. L. Cao, X. F. Long, G. S. Yang, N. Ye, $A(H_3C_3N_3O_3)(NO_3)$ (A = K, Rb): Alkali-Metal Nitrate Isocyanurates with Strong Optical Anisotropy, *Inorg. Chem.*, 2020, **59**, 10361–10367.
3. G. Peng, Y. Yang, Y. H. Tang, M. Luo, T. Yan, Y. Q. Zhou, C. S. Lin, Z. S. Lin, N. Ye, Collaborative enhancement from Pb^{2+} and F^- in $Pb_2(NO_3)_2(H_2O)F_2$ generates the largest second harmonic generation effect among nitrates, *Chem. Commun.*, 2017, **53**, 9398-9401.
4. Z. Y. Bai, K. M. Ok, Exceptional Optical Anisotropy Enhancement Achieved Through Dual-Ions Cosubstitution Strategy in Novel Hybrid Bismuth Halides, *Small*, 2024, 2311391.
5. Y. X. Song, M. Luo, C. S. Lin, N. Ye, Structural Modulation of Nitrate Group with Cations to Affect SHG Responses in $RE(OH)_2NO_3$ (RE = La, Y, and Gd): New Polar Materials with Large NLO Effect after Adjusting pH Values of Reaction Systems, *Chem. Mater.,* 2017, **29**, 896–903.
6. M. Cheng, W. Q. Jin, Z. H. Yang, S. L. Pan, Large optical anisotropy-oriented construction of a carbonate-nitrate chloride compound as a potential ultraviolet birefringent material, *Chem. Sci.*, 2022, **13**, 13482-13488.
7. L. Qi, X. X. Jiang, K. N. Duanmu, C. Wu, Z. S. Lin, Z. P. Huang, M. G. Humphrey, C. Zhang, Quadruple-Bidentate Nitrate-Ligated $A_2Hg(NO_3)_4$ (A=K, Rb): Strong Second-Harmonic Generation and Sufficient Birefringence, *Angew. Chem. Int. Ed.*, 2023, **62**, e202309365.
8. X. H. Dong, L. Huang, Q. Y. Liu, H. M. Zeng, Z. Lin, D. G. Xu, G. H. Zou, Perfect balance harmony in $Ba_2NO_3(OH)_3$: a beryllium-free nitrate as a UV nonlinear optical material, *Chem. Commun.*, 2018, **54**, 5792-5795.
9. Y. G. Shen, W. R. Niu, Y. J. Luo, Y. W. Zhou, X. L. Xue, L. Q. Liu, $(C_8H_6BrN_2O)NO_3$: A Hybrid Nonlinear Optical Crystal With an Appropriate Birefringence, *Adv. Optical Mater.,* 2024, **12**, 2400062.
10. X. F. Wang, Y. Li, Z. L. Chen, J. Lee, F. F. Zhang, K. R. Poeppelmeier, S. L. Pan, K. M. Ok, $Sr(NO_3)(NH_2SO_3)\cdot H_2O$: First Nitrate Sulfamate Revealing Remarkable Second Harmonic Generation and Optimized Birefringence, *Small Struct*. 2023, **4**, 2300274.
11. L. Wang, H. M. Wang, D. Zhang, D. J. Gao, J. Bi, L. Huang, G. H. Zou, Centrosymmetric $RbSnF_2NO_3$vs. noncentrosymmetric $Rb_2SbF_3(NO_3)_2$, *Inorg. Chem. Front.*, 2021, **8**, 3317-3324.
12. Y. X. Ma, C. L. Hu, B. X. Li, F. Kong, J. G. Mao, $PbCdF(SeO_3)(NO_3)$: A Nonlinear Optical Material Produced by Synergistic Effect of Four Functional Units, *Inorg. Chem.,* 2018, **57**, 11839–11846.